JBC Papers in Press. Published on November 8, 2011 as Manuscript M111.302588
The latest version is at http://www.jbc.org/cgi/doi/10.1074/jbc.M111.302588

The mycobacterial transcriptional regulator *whiB7* links redox homeostasis and intrinsic antibiotic resistance*

Ján Burian[1,2], Santiago Ramón-García[1,2], Gaye Sweet[1,2], Anaximandro Gómez-Velasco[2,3], Yossef Av-Gay[1,2,3] and Charles J. Thompson[1,2]

[1]From the Department of Microbiology and Immunology and the [2]Centre for Tuberculosis Research, University of British Columbia, Vancouver, British Columbia, Canada, V6T 1Z3

[3]From the Department of Medicine, Division of Infectious Diseases, University of British Columbia, Vancouver, British Columbia, Canada

*Running Title: *Insights into whiB7 activation and action*

To whom correspondence should be addressed: Charles J. Thompson. Department of Microbiology and Immunology and the Centre for Tuberculosis Research, University of British Columbia, Vancouver, British Columbia, Canada, V6T 1Z3, Tel.: (604) 822-2501; Fax: (604) 822-6041; E-mail: charles.thompson@ubc.ca;

Keywords: *whiB7*; mycothiol; antibiotic resistance

Background: The *whiB7* gene is a multidrug resistance determinant in mycobacteria.
Results: WhiB7 autoregulates its own promoter in response to both antibiotics (in a structure and target independent manner) and to redox changes.
Conclusion: WhiB7 links cell metabolism, redox homeostasis, and antibiotic resistance.
Significance: Understanding antibiotic-induced metabolic stress responses in mycobacteria may lead to therapies for mycobacterial diseases including tuberculosis.

SUMMARY

Intrinsic drug resistance in *Mycobacterium tuberculosis* limits therapeutic options for treating tuberculosis. The mycobacterial transcriptional regulator *whiB7* contributes to intrinsic resistance by activating its own expression and many drug resistance genes in response to antibiotics. To investigate *whiB7* activation, we constructed a GFP reporter to monitor its expression, and used it to investigate the *whiB7* promoter and to screen our custom library of almost 600 bioactive compounds including the majority of clinical antibiotics. Result showed *whiB7* was transcribed from a promoter that was conserved across mycobacteria and other actinomycetes including an AT rich sequence that was likely targeted by WhiB7. Expression was induced by compounds having diverse structures and targets, independent of the ability of *whiB7* to mediate resistance, and was dependent on media composition. Pretreatment with *whiB7* activators resulted in clinically relevant increases in intrinsic drug resistance. Antibiotic-induced transcription was synergistically increased by the reductant dithiothreitol, an effect mirrored by a *whiB7*-dependent shift to a highly reduced cytoplasm reflected by the reduced:oxidized mycothiol ratio. These data provided evidence that intrinsic resistance resulting from *whiB7* activation is linked to fundamental changes in cell metabolism.

The continued rise and prevalence of antibiotic resistance has progressively limited the use of available antibiotics and highlighted a need for new directions in the search for novel and effective antimicrobial therapies (1). Antibiotic resistance is typically mediated by proteins that are transcriptionally activated in response to drug exposure. Chemical inhibitors of drug-activated regulatory proteins or the products of corresponding resistance genes can potentiate antibiotic activity (2,3). Studies of antibiotic activities have traditionally focused on their abilities to inhibit specific targets essential for

bacterial growth including cell wall biosynthesis, transcription, translation, or DNA replication, with the implicit assumption that these are the direct causes of growth arrest or cell death (4). However, antibiotics exert diverse secondary effects that might provide signals of metabolic distress. In *Escherichia coli*, antibiotics that inhibit ribosomal function induce heat or cold shock responses (5). Importantly, antibiotics alter cell metabolism by activating transcription of up to one in twenty promoters in a concentration- and medium-dependent manner (6). These global changes of gene expression can help predict an antibiotic's mode of action (7). Furthermore, recent studies indicate that oxidative stress induced by bactericidal antibiotics might be a common cause of cell death (8). Understanding the activation and function of the global response to antibiotic exposure may provide new strategies to overcome antibiotic resistance.

Mycobacterium tuberculosis, the etiologic agent of tuberculosis, is intrinsically resistant to most clinically available antibiotics. Intrinsic resistance systems include the low permeability of the cell envelope, drug exporters, drug modifying systems and target modifying enzymes (2). Intrinsic antibiotic resistance to any given drug may be determined by an interactive network including effector proteins, regulatory proteins, and inducers (9). WhiB7, the focus of our study, is a transcriptional regulator of genes that contribute to intrinsic antibiotic resistance in mycobacteria (10).

The WhiB-family of transcriptional regulators is found only in actinomycetes. These include benign and pathogenic mycobacteria as well as *Streptomyces*, producers of the majority of known antibiotics. In mycobacteria, the WhiB-family has vital roles in fundamental cell processes including cell division, redox homeostasis, virulence, and antibiotic resistance (10-12). Little is known about the signals that activate transcription of the *whiB* genes.

Upon antibiotic treatment, *whiB7* has an essential role in activating transcription of antibiotic resistance systems for tetracyclines, macrolides, lincosamides and aminoglycosides (10). Transcription of *whiB7* is induced by antibiotic treatment as well as a variety of stress conditions such as heat shock, iron starvation and entry into stationary phase (13). Importantly, *whiB7* is highly induced in clinical isolates of the *M. tuberculosis* complex soon after infection of resting and activated murine macrophages (14). The observation that constitutive expression of *whiB7 in trans* activated transcription of its native genomic allele suggested autoregulation (10). Like other WhiB proteins, WhiB7 contains 4 cysteine residues that can either bind an iron sulfur cluster or form disulfide bridges within the apo-protein (15). WhiB proteins are redox sensitive and play critical roles in transcriptional activation (12,16,17). Here we identify the essential motifs of *whiB7*-dependent promoters and explore the mechanism by which the WhiB7 protein responds to diverse antibiotics and physiologies to activate expression of intrinsic drug resistance genes.

EXPERIMENTAL PROCEDURES

Bacterial strains and culture conditions- *Escherichia coli* TOP10 (Invitrogen) was used for cloning. It was cultured in LB broth (Sigma) supplemented with appropriate antibiotics shaking at 200 rpm, 37 ºC. Unless otherwise specified, *Mycobacterium smegmatis* mc^2155 was cultured in Middlebrook 7H9 broth (Difco) supplemented with 10 % ADC, 0.2 % (v/v) Glycerol, 0.05 % Tyloxapol, and appropriate antibiotics at 37 ºC either shaking in flasks at 200 rpm or rolling in test tubes. Kanamycin was used at a final concentration of 30 μg/mL, hygromycin at 50 μg/mL, apramycin at 50 μg/mL and ampicillin at 200 μg/mL.

Cloning- All PCR was performed using Dynazyme EXT (NEB F-505S) according to manufacturer instructions. Reactions included 5 % (v/v) dimethyl sulfoxide. Restriction enzymes were from New England Biolabs; digests were preformed according to manufacturer instructions. Ligations were performed using T4 DNA ligase (Invitrogen #15224-041) overnight at 16 ºC. Strain and plasmid constructions are summarized in Table 1. Oligonucleotides used are listed in Table S1.

Construction of the Lux reporters- A DNA fragment containing nucleotides +2 to +674 upstream of the annotated start codon of *whiB7 (Rv3197a)* was amplified from *Mycobacterium tuberculosis* H37Rv genomic DNA by PCR using the primers TBpromF and TBpromR. The fragment was digested with *Acl*I and *Eco*RI and cloned into pMV361 digested with the same

enzymes to create pMV361-P_{B7TB}. The *Eco*RI fragment containing the *luxABCDE* genes was isolated from pAmilux (18) and cloned into *Eco*RI digested pMV361 and pMV361-P_{B7TB} to create the HSP60 promoter driven, constitutively active pLUXon and the antibiotic inducible, *whiB7* promoter driven pTB674lux, respectively.

Construction of the GFP reporters- A DNA fragment containing the *egfp* gene from pEGFP (Clontech) was amplified by PCR using the primers eGFP_F and eGFP_R. The fragment was cloned, using the polymerase added A overhang, into pGEM-Teasy (Promega) to create pAB2. A DNA fragment containing the first three amino acids of the annotated *whiB7 (MSMEG_1953)* and 689 nucleotides upstream region was amplified from the genome of *Mycobacterium smegmatis* mc^2155 by PCR using the primers smegpromF and smegpromR. The fragment was cloned into pGEM-Teasy to create pAB6. pAB6 was digested with *Cla*I and *Hind*III and the *whiB7* promoter containing fragment was cloned into pMycVec1 digested with the same enzymes to create pAB7. pAB2 was digested with *Hind*III and *Xba*I and the *egfp* containing DNA fragment was cloned into pAB7 digested with the same enzymes to create antibiotic inducible, *whiB7* promoter driven pMS689GFP.

The *efgp* from pMS689GFP was amplified by PCR using the primers HSPGFP_F and HSPGFP_R. The PCR fragment was digested with *Bam*HI and *Eco*RI and cloned into pMV261 digested with the same enzymes, to create the HSP60 promoter driven, constitutively active pGFPon.

Sub-cloning the GFP reporter promoter- Shorter fragments of the upstream *whiB7* region were amplified from pMS689GFP. The PCR product of GFPsub_R and 438_F was digested with *Acl*I and cloned into *Cla*I and *Eco*RV digested pMycVec1 to create pMS438GFP. The PCR products of 497_F and 483_F in combination with GFPsubX_R were digested with *Cla*I and *Xba*I and cloned into *Cla*I/*Xba*I digested pMycVec1 to create pMS497GFP and pMS483GFP, respectively.

Complementation of whiB7 KO strain- The *whiB7* gene including its 520 bp upstream and 152 bp downstream regions was amplified by PCR from the *M. smegmatis* genome using primers B7comp_F and B7comp_R. The PCR fragment was cloned into pMV361, replacing the HSP60 promoter, using *Xba*I and *HindIII* to construct p361comp. A 1347 bp region of pAB707 containing the apramycin resistance gene *aac(3)IV* was amplified by PCR using the primers 707apra_F and 707apra_R. The product was cloned into p361comp using *Hind*III and *Spe*I to construct p361comp.apra. The integrative p361comp.apra was then used to complement the pMS689GFP containing *M. smegmatis whiB7* KO.

Construction of the ermMT over-expression strain- Rv1988 (*ermMT)* was amplified from *M. tuberculosis* H37Rv genomic DNA by PCR using the primers Rv1988_F and Rv1988_R. The PCR product was digested with *Eco*RI and *Hind*III, and cloned into pMV361 digested with the same enzymes. The resulting vector was digested with *Mfe*I and *Cla*I, and the *ermMT* containing fragment was cloned into pMV361.hyg digested with the same enzymes to create pERM.hyg. *M. smegmatis* was transformed with the plasmid, transformants were selected for by hygromycin and an increased resistance to macrolides was checked.

Luminescence Timecourse- M. smegmatis harbouring pTB7lux was inoculated into 3 mL of 7H9 + kanamycin and grown for 55-60 hours, followed by an incubation at room temperature for 12-15 hours. The culture was diluted to an OD600 nm of 0.01-0.005 into 3 mL of kanamycin free 7H9 and grown to an OD600 nm of 0.6-0.8, ~20-24 hours. Finally, the culture was diluted to an OD600 nm of 0.2 and 200 µL was distributed into a black, clear bottom 96 well plate (Costar 3631). The appropriate compound was added to the desired concentration and the plate was placed immediately into a VarioskanFlash (Thermo Scientific). Using the SkanIt RE 2.4.3 software the VarioskanFlash was set to raise the temperature to 37 ºC and without waiting shook the plate for 15 seconds at 420 rpm, followed by measuring the OD600 nm and finally measuring luminescence for 1000 ms. The shaking, OD reading and luminescence reading was repeat 12 times at 30 minute intervals, three times at 1 hour intervals, and finally, twice at 3 hour intervals. *M. smegmatis* wild type and *whiB7* KO harbouring pLUXon were prepared in identical fashion but diluted to an OD600 nm of 0.2 after the room temperature incubation and the timecourse run.

Fluorescence Timecourse- M. smegmatis harbouring pMS689GFP was inoculated into 3mL of 7H9 + kanamycin and grown for 48-54 hours until a final OD600 nm of 6-8. The culture was diluted to an OD600 nm of 0.01-0.005 into 3mL of kanamycin free 7H9 and grown to an OD600 nm of 0.6-0.8, ~20-24h. Finally, the culture was diluted to an OD600 nm of 0.2 and 200 µL was distributed into a black, clear bottom 96 well plate. The appropriate compound was added to the desired concentration and the plate was covered with Microseal® 'B' Film (BioRad MSB1001), placed immediately into a VarioskanFlash, and fluorescence was monitored. Briefly, the temperature was raised to 37 ºC and without waiting the plate was shaken for 15 seconds at 420 rpm, followed by measuring the OD600 nm and finally measuring fluorescence under default settings by excitation at 488nm and measuring emission at 509nm. The shaking, OD measurement and fluorescence measurement was repeated every 30 minutes 30 more times. *M. smegmatis* wild type and *whiB7* KO harbouring pGFPon was prepared in identical fashion but diluted to an OD600 nm of 0.2 after the 48-54 hour incubation and the timecourse run.

WhiB7 activation assay- M. smegmatis harbouring pMS689GFP was inoculated into 3mL of 7H9 + kanamycin and grown for 48-54 hours to a final OD600 nm of 6-8. The inoculum was diluted to an OD 600nm of 0.0125 in 50mL of kanamycin free 7H9 and grown for ~20 hours to an OD 600nm of 0.6-0.8. The culture was diluted to an OD600 nm of 0.2 and dispensed into a black, clear bottom 96 well plate. Wells 1-11 of row A received 300 µL and the rest of the plate received 200 µL, except for wells in column 12 of row G and H which received 200 µL of sterile media. For the wells that received 300 µL of culture, 3 µL of stock 5 mM compounds was added and 100 µL was used to serially dilute down from row A to row H creating a concentration range of 50 µM to 0.02 µM in a final volume 200 µL. The plate was covered with a lid, wrapped in tin foil, and incubated at 37 ºC, 200 rpm for 5 hours. After the incubation the plate was placed in a VarioskanFlask, the OD600 nm and emission at 509 nm after 488 nm excitation were measured following a shaking for 15 seconds at 420 rpm. The assay is presented graphically in Figure S4. The OD and fluorescence values were corrected by subtracting the average of the values measured in wells 12 of row G and H (sterile media). The fluorescent values were then standardized to the OD by dividing the fluorescent value of a well by its corresponding OD value. Finally the fold increase of standardized fluorescence was calculated by dividing values by the average of the untreated wells (wells 12 of row A to F). Because EGFP continued to fluoresce in cultures whose OD_{600} had been reduced by antibiotic-induced lysis (data not shown), wells with an OD_{600} less than one third of the untreated wells were disregarded. The concentration range for each compound was analysed in three biologically independent runs. A compound was considered a WhiB7 activator if there was at least a ≥4 fold increase in fluorescence versus the untreated control in two out of the three replicates.

MIC determination- M. smegmatis wild type or *whiB7* KO was inoculated into 3 mL of 7H9 and grown for 48-54 hours to a final OD600 nm of 6-8. The culture was diluted to an OD 600nm of 0.005 and 100 µL was added to 100 µL of antibiotic containing 7H9 at two-fold serial dilutions across a 96 well plate (Costar 3370). The plate was incubated for 48 hours and 30 µL of sterile 10 mg/100mL (w/v) Rezazurin solution was added and the plate was incubated for an additional 24 hours. Wells which remained blue were deemed to contain an inhibitory concentration of antibiotic.

mRNA isolation and quantification- M. smegmatis was grown to an OD600 nm of 0.6-0.8 and split into 30-50 mL aliquots. The appropriate amount of antibiotic was added to selected aliquots and the cultures were incubated for 1 hour. Four times culture volume of GTC buffer (5 M guanidine thiocyanate , 17 mM sodium lauroyl sarcosinate, 28.5 mM trisodium citrate, 0.5 % (v/v) Tween 80, 0.7 % (v/v) 2-Mercaptoethanol) was added and the samples were incubated for 1 hour at room temperature. Samples were pelleted by centrifugation for 10 minutes, 5000 rpm, 4 ºC and the supernatant discarded. The pellets were suspended in 1mL QIAzol (Qiagen #79306) and transferred to a 2 mL screw cap tube (MBP #3488) containing ~100 µL of 0.1 mm glass beads (BioSpec #11079101). The tubes were beaten three times using a MP FastPrep-24 at 6.0 m/s for 45 seconds with 3-5 minute ice breaks. The

samples were centrifuged for 5 minutes at 16,000 g, 4 ºC and the supernatants were transferred to phase gel lock tubes (5 Prime #2302830). The tubes were incubated at room temperature for 5 minutes and 0.2 mL of ice cold chloroform was added. The tube contents were mixed by inversion for 15 seconds, incubated at room temperature for 3 minutes and finally centrifuged for 5 minutes at 16,000 g, 4 ºC. The upper fraction was transferred to a 1.5 mL eppendorf containing 550 µL of 30 mM sodium acetate in isopropanol, mixed well, and incubated overnight at -20ºC. The samples were centrifuged for 10 minutes at 16,000 g, 4 ºC, the supernatant discarded, and the pellets were washed with 1 mL ice cold 75 % (v/v) ethanol. Samples were centrifuged for 5 minutes at 16,000 g, 4 ºC and the supernatant discarded. The pellets were dissolved in 90 µL RNase free water by incubation at 65 ºC for 10 minutes. Samples were then treated for 30 minutes at 37 ºC with Turbo DNase (Ambion #AM2239) and finally the RNA was isolated by RNAspin mini columns (GE #25-0500-72) according to manufacturer instructions.

The qScript cDNA synthesis kit (Quanta #95047-100) was used to reverse transcribe a total of 100 ng of RNA per 20 µL reaction [25 ºC – 5 minutes, 42 ºC – 30 minutes, 85 ºC – 5 minutes]. The cDNA samples were diluted 1/10 and 2.5 µL was used per 25 µL quantitave PCR rection. A mix of PerfeCTa SYBR green supermix (Quanta #95054-050), cDNA and primers (1 µM each) was run on a BioRad Opticon2 [95 ºC – 3 minutes, 95 ºC – 30 seconds, 55 ºC – 30 seconds, 72 ºC – 30 seconds, read, repeated from step two 34 times]. A standard curve of genomic DNA was used calculate concentrations, and a non-reverse transcribed control to estimate DNA contamination. Primers used for *whiB7* were prAB47a and prAB48. Concentrations were standardized to an internal control, *mysA*, using primers prAB49 and prAB50. Fold increase of *whiB7* was calculated against a non-treated sample run in parallel.

Transcription start site determination- Transcriptional start site of the antibiotic induced *whiB7* promoter was identified by essentially unmodified Directed Mapping of Transcription Start Site (DMTSS) method developed by Mendoza-Vargas *et al*. (19). Briefly, RNA was isolated from retapamulin treated *M*. *smegmatis* by the method mentioned above. About 1.5 µg total RNA was mixed with 700 pmol of a radom hexamer primer (NNNNNN) and the solution was heated to 70 ºC for 10 minutes followed by incubation on ice for 5 minutes. cDNA was generated using Transcriptor reverse transcriptase (Roche 03 351 317 001) according to manufacturer instruction [25 ºC – 20 minutes, 60 ºC – 40 minutes, 85 ºC – 5 minutes] and isolated by the QIAquick PCR purification kit (Qiagen 28106). A guanine tail was added to the 3' end of the cDNA library using Terminal transferase (Roche 03 333 566 001) according to manufacturer's instruction [37 ºC – 30 minutes, 70 ºC – 10 minutes] and the cDNA was once again isolated by the QIAquick PCR purification kit. Linear amplification of the tailed cDNA library was carried out using Dynazyme EXT in combination with the enrich_C primer [94 ºC – 10 minutes, 94 ºC – 1 minute, 50 ºC – 1 minute, 72 ºC – 3 minutes, repeated from step two 34 times, 72ºC – 10 minutes) and the cDNA was isolated by the QIAquick PCR purification kit. About 15 ng of the DNA was used per 50 µL PCR reaction using Dynazyme EXT with primers TSS_adaptor and whiB7_TSS58 (94 ºC – 3 minutes, 94 ºC – 30 seconds, 60 ºC – 10 seconds, 72 ºC – 30 seconds, repeated from step two 34 times, 72 ºC – 5.5 minutes). A single PCR product of about 200 bp was observed by agarose gel electrophoresis. This product was cloned, using the polymerase added A overhang, into pGEM-Teasy and transformed into *E*. *coli* TOP10. Several white transformants visualized on LB+ampicillin+ 20 µg/mL Xgal+ 0.1 mM IPTG agar plates were transferred to liquid media, and plasmid DNA was isolated using the QIAprep Spin Miniprep Kit (Qiagen 27106). The plasmids were sent for sequencing at the UBC Vancouver campus NAPS unit (http://naps.msl.ubc.ca/) using the M13R primer.

Analysis of mycothiol content- M. *smegmatis* wild type or *whiB7* KO was grown in 100 mL of NE (glucose 10 g/L, yeast extract 2 g/L, casaminoacids 2 g/L, lab lemco powder 1 g/L) supplemented to 0.05% Tyloxapol at 37 ºC, 200 rpm to an OD_{600} of 2.0. Cultures were then divided into two 50 mL fractions and one fraction received erythromycin to a final concentration of 256 µg/mL. All fractions were further incubated at 37 ºC for 1 hour. Growth was arrested by the addition of an equal volume of pre-chilled water. The fractions were then divided for centrifugation at

4˚C; 10 mL for MSH determination, 30 mL for MSSM determination, and 5 mL for NEM labeling (negative control). Pellets were flash-frozen in liquid nitrogen and stored at -80˚C until analysis. HPLC analysis of MSH levels was performed as previously described (20).

Nicotinamide adenine dinucleotide quantification- *M. smegmatis* wild type or *whiB7* KO was grown in 50 mL of NE supplemented to 0.05% Tyloxapol at 37 ºC, 200 rpm to an OD_{600} of 2.0. Cultures were then divided into two 25 mL fractions and one fraction received erythromycin to a final concentration of 256 µg/mL. All fractions were further incubated at 37 ºC for 1 hour and samples taken. Erythromycin treated samples were left to incubate for an additional 1 hour for the 2 hour time point. Concentrations of reduced (NADH) and oxidized (NAD+) forms of nicotinamide adenine dinucleotide were analyzed as previously described (21). Once samples were extracted the enzymatic reaction was carried out in a black, clear bottom 96 well plate (Costar 3631). Samples and standards were analyzed in triplicate, and only 6 wells were prepared and followed at one time. The Varioskan was set to read the absorbance (570nm) every 20 seconds for 5 minutes. Concentrations were calculated from a standard curve (R^2 = 0.9996) of NADH (Sigma N6660-15VL) and standardized to dry weight per litre of culture.

RESULTS

Fluorescent and luminescent reporters to study whiB7 promoter activity- Enhanced green fluorescent protein (EGFP) and bacterial luciferase (LuxABCDE) were evaluated as reporters to study the *whiB7* promoter and its response to diverse drugs. qRT-PCR confirmed that *whiB7* transcription was activated in *M. smegmatis* by erythromycin [an inducer of *whiB7* in *M. tuberculosis*, (10)], but not isoniazid (Table 2). To monitor the promoter controlling the *M. smegmatis whiB7* gene, plasmid pMS689GFP was constructed; it encodes the first 9 base pairs of *whiB7* and the 689 nucleotide upstream region (i.e., the entire 513 bp intergenic region and the last 176 bp of the proximal upstream gene, *uvrD2*) fused to EGFP. An alternative reporter plasmid was also constructed (pTB674lux) containing the upstream intergenic region of the *M. tuberculosis whiB7* gene fused to the *luxABCDE* reporter system. To determine whether these constructs contained the antibiotic inducible *whiB7* promoter, erythromycin or isoniazid were added to cultures of *M. smegmatis* containing pMS689GFP (Figure 1A) or pTB674lux (Figure 1B). Erythromycin, but not isoniazid, induced signal in these cultures. Both *whiB7* promoter reporter systems consistently displayed similar induction kinetics, resulting in 4-6 fold increases in signal after 3 hours of induction with erythromycin (Figure 1). Furthermore, the level of erythromycin-induced pMS689GFP fluorescence was much lower in a *whiB7* mutant (Figure 1C; *whiB7* KO) but was restored upon complementation (Figure 1D). This demonstrated that pMS689GFP could be used to monitor antibiotic-induced transcriptional activation of the *whiB7* promoter and provided further evidence that WhiB7 played an essential role in activating its own promoter.

To test whether the EGFP or LuxABCDE reporter activities might be dependent on *whiB7*, both reporters were expressed constitutively from the *M. tuberculosis* HSP60 promoter (constructs pGFPon and pLUXon) in *M. smegmatis* wild type or *whiB7* KO strains. As expected, pGFPon generated indistinguishable levels of fluorescence in wild type and *whiB7* KO strains (Figure 1E). In contrast, light output by pLUXon was much lower in the *whiB7* KO strain background (Figure 1F). This surprising observation revealed that optimal light production by the LuxABCDE protein complex was dependent on physiological conditions determined by *whiB7*. In addition, a limited screen of our antimicrobial compounds revealed that at least one drug, the IκB-α phosphorylation inhibitor BAY 11-7085, abolished bioluminescence from both pTB674lux and pLUXon in *M. smegmatis* at concentrations below its minimum inhibitory concentration (MIC) (Figure S1). These results showed that the LuxABCDE reporter system was dependent on *whiB7* and that anti-microbial compounds could also have direct or indirect inhibitory effects on its activity. While these observations may lead to future insights into the role of *whiB7* or drugs on mycobacterial physiology, it was clear that pTB674lux was not a suitable reporter of *whiB7* promoter activity and pMS689GFP was chosen to monitor *whiB7* transcriptional activation.

Mapping the antibiotic-responsive whiB7 promoter region- An alignment of the sequences

upstream of *whiB7* in the genomes of various *Mycobacterium* species revealed conserved sequences resembling promoter (-10 and -35) hexamers and an AT-rich region (Figure 2A). This motif was located between nucleotides 438 and 497 upstream of the annotated *M. smegmatis whiB7* gene. To determine whether this region contained the inducible *whiB7* promoter, the 689 bp upstream sequence used to construct pMS689GFP was shortened to 497 (pMS497GFP), 483 (pMS483GFP), or 438 (pMS438GFP) nucleotides. Only pMS497GFP responded similarly to pMS689GFP when treated with erythromycin (Figure 2B). This was also observed using a broad range of *whiB7* activators including retapamulin, tilmicosin, doxycycline, linezolid, A23187 and acivicin (Figure S2). A considerably reduced fluorescence response was generated by pMS483GFP, a construction lacking the conserved AT-rich region (Figure 2B), whereas no fluorescence was detected with pMS438GFP lacking the putative *whiB7* promoter (Figure S3).

The transcriptional start site of the antibiotic-induced *whiB7* promoter was mapped to a position 445 nucleotides upstream of the gene (Figure 2C). The region contained the predicted *whiB7* promoter and this conserved motif was identified upstream of *whiB7* in 12 representative actinomycete genera (KEGG database: http://www.genome.jp/kegg; Figure 2D). In all cases, there was an AT-rich region three bases upstream of the conserved -35 site, TTGNNN, and a conserved -10 site, TANNNT. The AT-rich motif was present three bases upstream of the well characterized *eis* promoter (22), and also upstream of other genes within the *whiB7* regulon (*tap* and *ermMT*) (10) (Figure 2E).

Activation of the whiB7 promoter is independent of antibiotic structure, primary target of inhibition, and the ability of whiB7 to mediate resistance- To investigate *whiB7* transcriptional activation, a custom compound library (Sweet library) was assembled and screened using the pMS689GFP reporter system. The 591-compound library (listed in Table S2) included the majority of commercially available antibiotics targeting DNA, RNA, protein, cell envelope synthesis, or essential metabolic conversions, as well as other physiologically active compounds. Unlike other chemical libraries that are dissolved exclusively in dimethyl sulfoxide, each compound in the Sweet library was dissolved in an optimal solvent (water, dimethyl sulfoxide, ethanol, methanol, or dimethylformamide) to ensure solubility and maximize hit discovery. A semi-high throughput screen was devised to assay the library for activators of *whiB7* transcription. Each compound was serially diluted in 96 well plates in order to survey a broad (2,500 fold) concentration range (50 μM to 0.02 μM; Figure S4). pMS689GFP fluorescence was monitored after 5 hours, when the culture had reached a plateau of signal intensity (Figure 1A). Hits were identified as compounds that induced a $\geq$ 4 fold increase in fluorescence in at least two out of three trials. In total, 86 *whiB7* activators were identified (Table S2). The reliability of the screen was validated by qRT-PCR analysis of 23 representative hits confirming that all induced *whiB7* transcription (Figure 3 and Table S2), while 4 non-hits did not (Table S2).

Structure clustering analyses (http://pubchem.ncbi.nlm.nih.gov/assay/assay.cgi?p=clustering) allowed visualization of potential similarities in the chemical structures of *whiB7* activators (Figure 3). Compounds with statistically similar structure, suggesting similar bioactivities, are defined by a Tanimoto score greater than 0.7 (23). The cluster analysis identified groups of active compounds having similar structures (including macrolides, aminoglycosides, fluoroquinolones and tetracyclines). However, the structural similarity between these major clades, as well as most of the other activators, was well below 0.7. Therefore, *whiB7* transcriptional activation was not due to a common structural motif of the compounds.

The structural diversity of the identified activators was also reflected in the diversity of their documented targets. Half of the identified *whiB7* activators, including macrolides, tetracyclines, lincosamides, and aminoglycosides, inhibited protein synthesis, targeting different sites within the 50S or the 30S subunits of the ribosome. The second major target was DNA replication, which was inhibited by fluoroquinolones and DNA intercalators including netropsin, nogalamycin, and phleomycin. Other potent activators (including acivicin, dequalinium, beauvericin, and A23187) are known for their pleiotropic effects on cell metabolism. These data showed that induction of *whiB7* transcription did

not result from direct inhibition of a single target or function, and implied a common, downstream effect of the activators on metabolism. Curiously, cell wall biosynthesis inhibitors, including the extended family of beta-lactams, did not induce transcription.

To provide further evidence for the concept that direct recognition of antibiotic structure was not needed for *whiB7* activation, the *M. tuberculosis* ribosomal methyltransferase (encoded by *ermMT*) that confers macrolide resistance by preventing interaction between macrolide and its ribosomal target (24), was constitutively expressed from the HSP60 promoter in *M. smegmatis* (*ermMT* OE). If the *whiB7* promoter was induced in response to macrolide structure, independent of translation inhibitory effects, the level of pMS689GFP activation would be the same in wild type and in the *ermMT*-expressing, resistant strain. Alternatively, if *whiB7* transcription responded to the stress generated by toxic macrolide-ribosome interactions, macrolides would elicit reduced *whiB7* activation in the resistant strain. When *M. smegmatis ermMT* OE/ pMS689GFP was exposed to various macrolides (erythromycin, dirithromycin, roxithromycin, or azithromycin) at concentrations that activated pMS689GFP in the wild type background, the level of induced fluorescence was ~5 fold lower (Figure 4). The level of activation by doxycycline, an antibiotic whose activity is unaffected by ErmMT, was unchanged (Figure 4).

Interestingly, several activators were not within the *whiB7* sensitivity spectrum. For example, while dequalinium, linezolid, danofloxacin, and A23187 were all active inducers of *whiB7* expression, the *whiB7* KO mutant was not more sensitive to these compounds (Table 2). Furthermore, pre-treatment with *whiB7* inducers increased intrinsic resistance levels. Pre-treatment with sub-inhibitory concentrations of erythromycin or clarithromycin increased resistance to those antibiotics in a *whiB7*-dependent manner (Table S3). Similarly, treatment with acivicin, an amino acid analog, also increased resistance to macrolides (4-fold; Table S4).

The fact that the glutamine analog acivicin was a strong inducer of *whiB7* transcription (Table 2), suggested a link between amino acid metabolism and *whiB7* activation. When glutamate, the only amino acid in standard 7H9 medium, was either retained or replaced with glutamine, aspartate, asparagine, arginine, or histidine, and cultures were treated with erythromycin, levels of *whiB7* induction varied; induced levels were similar in cultures grown in the presence of glutamate, aspartate or histidine, whereas increased levels of induction were observed in cultures grown in the presence of asparagine with a limited increase with glutamine and a possible small increase with arginine (Figure S6).

Redox state modulates the level of whiB7 transcriptional activation- Based on *in vitro* studies showing that WhiB proteins, including WhiB7, have oxygen sensitive iron sulphur clusters (12,15) that may affect transcription (17), and our studies establishing that *whiB7* is needed for regulation of its own promoter, experiments were carried out to explore the hypothesis that oxidizing or reducing reagents (diamide or dithiothreitol (DTT)) might affect *whiB7* promoter activity *in vivo*. In the absence of erythromycin, the thiol reductant DTT moderately induced expression (Figure 5A). Treatment with DTT in combination with a low dose of erythromycin generated a strong, synergistic (~1,300 fold) increase in mRNA levels (Figure 5A). Conversely, the thiol oxidant diamide generated a negligible increase in *whiB7* mRNA and decreased the level of induction by erythromycin approximately 5 fold (Figure 5A). These data indicate that a reduced state favors *whiB7* transcriptional activation.

Kohanski *et al*. (8) reported that hydroxyl radical formation is a common mechanism of antibiotic-mediated bacterial cell death. Because our experiments demonstrated that reducing, rather than oxidizing, conditions enhanced *whiB7* activation, it seemed unlikely that *whiB7* transcription was responding to hydroxyl radicals generated by antibiotic action. In fact, adding the hydroxyl scavenger thiourea at concentrations similar to those used by Kohanski *et al*. to prevent significant hydroxyl radical accumulation, did not prevent *whiB7* transcriptional activation by several antibiotics (Figure S5). Instead, thiourea activated the pMS689GFP reporter (Figure S5). This provided further evidence that *whiB7* activation is intimately linked with cell metabolism and activated by a reducing environment.

Mycothiol, the major low molecular weight reducing agent in actinomycetes, provides resistance to free radicals as well as antibiotics

(25,26). In mycobacteria, the ratio between its reduced form (MSH) and its oxidized disulfide form (MSSM) serves as an indicator of intracellular redox potential, with a basal reducing ratio of about 200:1 (MSH:MSSM) in *M. smegmatis* (20). Without an antibiotic inducer, the *whiB7* KO contained ~10 fold less MSH and ~2 fold less MSSM (Figure 5B) than the wild type, reflecting in a ~5 fold decrease in MSH:MSSM (Figure 5C). After treatment with erythromycin, MSH levels were unchanged in wild type cells or the *whiB7* KO background (Figure 5B). Importantly, erythromycin treatment virtually eliminated detectable MSSM in wild type cells and had no effect on levels in the *whiB7* KO (Figure 5B). This resulted in a ~180 fold MSH:MSSM increase in wild type cells (Figure 5C).

To determine whether the reduced MSH:MSSM ratio in the *whiB7* KO or the increased MSH:MSSM ratio generated by treatment with erythromycin in the wild type reflected broader effects on redox metabolism, the levels of reduced (NADH) and oxidized (NAD+) nicotinamide adenine dinucleotide were quantified. During exponential growth the *whiB7* KO strains contained slightly lower levels (40% decreased) of NADH compared to wild type (Figure S7A). Upon erythromycin treatment, the levels of both NADH and NAD+ increased in both strains. The increase was more pronounced in the *whiB7* KO; after 2 hours of erythromycin treatment NADH levels increased ~3 fold and NAD+ levels ~2 fold, while the increases in wild type were ~1.6 and ~1.2 fold, respectively (Figure S7A). The NADH:NAD+ ratio was ~1.6 fold lower in the *whiB7* KO relative to wild type in exponentially growing cultures, and the ratio in both strains increased after erythromycin treatment (~1.3 and ~1.7 fold after two hours in the wild type and *whiB7* KO; Figure S7B).

DISCUSSION

To better understand factors that affect the intrinsic resistance of mycobacteria to antibiotics, we identified essential components of the *whiB7* promoter and the spectrum of inducers that activate its transcription using an EGFP reporter system. Our chemical screens and investigations of redox metabolism provided new insights into the biological activation of *whiB7* expression. We suggest that inducers generate a reductive shift of redox metabolism in response to inhibition of diverse cellular targets and that this leads to the transcriptional activation of *whiB7*-dependent intrinsic drug resistance.

Actinomycete genomes all encode WhiB7 orthologs as well as a conserved promoter consensus sequence (Figure 2D), suggesting that *whiB7* has an indispensible role in natural environments and that its transcriptional activation system is conserved in this diverse group of soil and pathogenic bacteria. A comparison of the *whiB7* promoter to consensus sequences for all *M. tuberculosis* sigma factors (27) showed that its -35 and -10 hexamer sequences and their spacing was most similar to SigA, the primary vegetative sigma factor. By analogy to WhiB3, WhiB7 may partner with SigA to activate transcription of specialized regulons (28). Since loss of the conserved AT rich region upstream of the -35 hexamer restricted activation (Figure 2B) and WhiB7 contains an AT-hook (10), a motif known to bind the minor groove of AT-rich DNA (29), our results imply that the sequence serves as a WhiB7 binding site. The recognition motif is also found upstream of the genes within the proposed regulon (Figure 2E). The *M. smegmatis* genome contains 5,954 regions with blocks of at least five adjacent A or T nucleotides (searched with '[AT]{5}' in DNA Pattern Search available at www.geneinfinity.org). Since many WhiB proteins do not encode an obvious AT hook motif, other conserved regions of WhiB7 may be involved in binding DNA directly or by partnering with other transcriptional activators to target promoters within its regulon. Although antibiotic induction of the *whiB7* promoter was strongly reduced in the *whiB7* KO background, a slow, constant increase in activity was observed (Figure 1E). This may reflect the participation of other regulatory elements that either repress under non-inducing conditions or co-activate upon induction.

The *whiB7* promoter was induced by a wide variety of compounds (Figure 3) at concentrations much lower than their MICs (Table 2). Many *whiB7* transcriptional activators perturb respiration, redox balance, or transmembrane ion flux. One of the most intriguing inducers was the glutamine analog acivicin. Acivicin inhibits glutamine amidotransferases leading to a response described as "metabolic mayhem" in *E. coli* (30). In our *M.*

smegmatis cultures, acivicin did not inhibit growth at the highest concentration tested (800 μM). The fact that it substantially increased *whiB7* transcription even at 16-fold lower concentrations (50 μM; Table S2) clearly illustrated the concept that activation was due to a drug-induced metabolic signal. The observation that not all toxic compounds induced *whiB7*, throughout a range of growth inhibitory and noninhibitory concentrations, demonstrated that the signal was not a common feature associated with cell death. Active compounds apparently induce a unique *whiB7*-specific metabolic stress signal. In fact, *whiB7* inducers were enriched for compounds that inhibit protein biosynthesis, demonstrated by a dose-dependent effect on ribosomes by macrolides (Figure 4; Figure 5A). Insights into specificity were also provided by the observation that none of the 50+ cell wall targeting compounds in the Sweet library induced *whiB7* expression (Table S2). Protein synthesis and cell wall inhibitors are known to induce distinctive stress signals associated with different stress regulons (31,32).

A previous study had demonstrated that treatment of *M. smegmatis* with sub-inhibitory concentrations of macrolides greatly increased resistance to these drugs in an *erm(38)* (the *M. smegmatis ermMT* ortholog; MSMEG_1646) - dependent manner (33). Our work showed that macrolide pre-treatment increased resistance to the activating macrolide in a *whiB7*-dependent manner (Table S3). The *whiB7* promoter motif was present upstream of *erm(38)* (Figure 2E) implying that the increase in resistance was mediated by *erm(38)* which requires *whiB7* for transcriptional activation. Therefore, a *whiB7* response to any activator compound or metabolic signal should similarly increase macrolide resistance. In support of this concept, our data demonstrated that pre-treatment with acivicin, a non-macrolide *whiB7* activator, resulted in increased resistance to macrolides (roxithromycin and clarithromycin; Table S4). The clinical relevance of this induced intrinsic resistance phenomenon has recently been demonstrated in multi-drug resistant strains of *M. tuberculosis*. Pre-treatment with rifampicin induced expression of multiple efflux pumps leading to increased resistance to ofloxacin, a quinolone (34). Rifampicin pre-treatment of these strains increased expression of *whiB7*, and presumably a multidrug transporter that it activates (*tap*, Rv1258c) contributing to the resistance state (10,34). These observations support a clinically important concept; exposure to *whiB7* inducers activates expression of genes and a metabolic state that provides cross-resistance to diverse drugs.

Since oxidative stress generated by hydroxyl radicals has been reported to be a common metabolic effect of cidal antibiotics in some bacteria (8), we monitored *whiB7* expression under reducing and oxidative culture conditions. Interestingly, DTT (providing additional reducing potential) activated a low level of *whiB7* transcription (Figure 5A). Combining reducing conditions with a low concentration of erythromycin synergistically increased *whiB7* transcription, mimicking treatment by a much higher concentration of erythromycin. In contrast, oxidizing conditions (diamide) decreased induction (Figure 5A). In addition, the hydroxyl radical scavenger thiourea did not prevent antibiotic-induced *whiB7* induction (Figure S5). This implied that the *whiB7* response to macrolides (and other drugs) was dependent on a metabolic shift to increased reducing potential that was generated independently of hydroxyl radical formation. The reducing potential of mycobacterial cells is reflected in the redox state of reducing agents including MSH and NADH.

Analyses of MSH, MSSH (Figure 5B), and their ratio (MSH:MSSM) (Figure 5C) revealed differences between wild type and *whiB7* KO strain, both untreated and in response to erythromycin. These studies revealed that *whiB7* participates in maintaining a reduced cytoplasmic (MSH:MSSM) environment under normal growth conditions and directly or indirectly controls the concentration of mycothiol (MSH+MSSM; Figure 5B). Furthermore, the fact that erythromycin treatment of the wild type strain resulted in a *whiB7*-dependent decrease in the pool of oxidized mycothiol suggested that WhiB7 had an active role in regulating MSSM reduction (Figure 5B). The decrease in MSSM shifted the MSH:MSSM ratio to a highly reduced state (Figure 5C). By analogy to other WhiB proteins, the activity of WhiB7 as a transcriptional activator may respond to such changes in the redox environment. In support of this model, DTT studies indicated that a highly reduced environment potentiated induction of *whiB7* transcription (Figure 5A). In contrast, erythromycin treatment of the *whiB7* KO did not

affect levels of oxidized mycothiol (Figure 5B) or its MSH:MSSM ratio (Figure 5C). By comparison, changes in NADH and NAD+ were relatively small, suggesting that the *whiB7*-dependent mycothiol redox changes were an initial response to erythromycin, reflected by slower changes in NADH/NAD+ pools. While increased NADH and NAD+ pools might be needed to provide longer term responses to erythromycin, they were metabolically isolated from MSH/MSSM pools under the condition of our experiment.

It has been reported that catabolism of host fatty acids in macrophages results in reductive stress by the accumulation of NADH/NADPH (12,35). The stress is dissipated by a WhiB3-dependent shift to the production of virulence lipids (12), but the initial reductive burst may explain the activation of *whiB7* in the *M. tuberculosis* complex soon after infection of macrophages (14) or in response to lipids added to the growth media (10). Additionally, macrophages also utilize glutathione as the major antioxidant for defence against *M. tuberculosis* infection (36). Exposure to glutathione may provide additional reductive stress to facilitate activation of *whiB7*. Finally, the observation that the *whiB7* KO strain has a more oxidized cytoplasm (Figure 5C) and lower levels of NADH (Figure S6A) rationalizes the reduced output of LuxABCDE bioluminescence (Figure 1D) which requires reducing power to generate reduced riboflavin mononucleotide, an essential cofactor for the light generating reaction (37).

Other transcriptional regulators containing redox sensitive disulfide bridges or iron-sulfur clusters serve to regulate critical redox responsive functions in bacteria (38). WhiB1, WhiB2, WhiB3, and WhiBTM4 (a bacteriophage encoded WhiB2-ortholog) proteins also interact with target promoters in a redox-sensitive manner (12,16,17). WhiB7, like all WhiB family proteins, contains 4 conserved cysteine residues that are able to bind a redox sensitive iron-sulfur cluster or form disulfide bonds. By analogy to biochemical studies of WhiB1, the iron-sulfur cluster-bound form of WhiB7 may be an inactive form of the protein that does not bind DNA (17). While our evidence supports the central role of reduced thiols, it does not necessarily rule out the involvement of oxidants. If oxidative damage is a common mechanism of bactericidal antibiotic mediated cell death (8), the cell may respond by shifting its redox balance back to a more reduced state. This might allow activation of WhiB7 to induce expression of other genes in its regulon and thereby generate a defensive response after exposure to some antibiotics.

Studies of antibiotic resistance in bacterial pathogens have traditionally focussed on genes carried by transmissible elements that provide drug resistance to pathogens. However, there is growing recognition that chromosomal genes having physiological functions can have alternative roles as antibiotic resistance genes. This new concept has important evolutionary implications, rationalizing the recruitment and evolution of metabolic genes to serve as antibiotic resistance genes or alternatively, to provide physiological functions for genes under selective pressure as resistance genes. Here we focused on *whiB7*, a transcriptional regulatory gene that determines intrinsic drug resistance in mycobacteria. Our studies revealed that WhiB7 is at a cross road between physiology and antibiotic resistance with functions linked to the maintenance of balanced reducing potential as well as activation of resistance genes. Activation of *whiB7* creates a non-specific resistance state that provides cross-resistance to diverse drugs. Understanding how WhiB7 senses antibiotic-induced signals to activate intrinsic resistance genes may allow more effective uses of drug combinations (39) for treatment of mycobacterial diseases including tuberculosis.

REFERENCES

1. Fischbach, M. A., and Walsh, C. T. (2009) *Science* **325**, 1089-1093
2. Nguyen, L., and Thompson, C. J. (2006) *Trends Microbiol* **14**, 304-312
3. Poole, K. (2001) *J Pharm Pharmacol* **53**, 283-294
4. Walsh, C. (2000) *Nature* **406**, 775-781
5. VanBogelen, R. A., and Neidhardt, F. C. (1990) *Proc Natl Acad Sci U S A* **87**, 5589-5593

6. Goh, E. B., Yim, G., Tsui, W., McClure, J., Surette, M. G., and Davies, J. (2002) *Proc Natl Acad Sci U S A* **99**, 17025-17030
7. Brazas, M. D., and Hancock, R. E. (2005) *Drug Discov Today* **10**, 1245-1252
8. Kohanski, M. A., Dwyer, D. J., Hayete, B., Lawrence, C. A., and Collins, J. J. (2007) *Cell* **130**, 797-810
9. Nishino, K., Nikaido, E., and Yamaguchi, A. (2009) *Biochim Biophys Acta* **1794**, 834-843
10. Morris, R. P., Nguyen, L., Gatfield, J., Visconti, K., Nguyen, K., Schnappinger, D., Ehrt, S., Liu, Y., Heifets, L., Pieters, J., Schoolnik, G., and Thompson, C. J. (2005) *Proc Natl Acad Sci U S A* **102**, 12200-12205
11. Gomez, J. E., and Bishai, W. R. (2000) *Proc Natl Acad Sci U S A* **97**, 8554-8559
12. Singh, A., Crossman, D. K., Mai, D., Guidry, L., Voskuil, M. I., Renfrow, M. B., and Steyn, A. J. (2009) *PLoS Pathog* **5**, e1000545
13. Geiman, D. E., Raghunand, T. R., Agarwal, N., and Bishai, W. R. (2006) *Antimicrob Agents Chemother* **50**, 2836-2841
14. Homolka, S., Niemann, S., Russell, D. G., and Rohde, K. H. (2010) *PLoS Pathog* **6**, e1000988
15. Alam, M. S., Garg, S. K., and Agrawal, P. (2009) *FEBS J* **276**, 76-93
16. Rybniker, J., Nowag, A., van Gumpel, E., Nissen, N., Robinson, N., Plum, G., and Hartmann, P. (2010) *Mol Microbiol* **77**, 642-657
17. Smith, L. J., Stapleton, M. R., Fullstone, G. J., Crack, J. C., Thomson, A. J., Le Brun, N. E., Hunt, D. M., Harvey, E., Adinolfi, S., Buxton, R. S., and Green, J. (2010) *Biochem J* **432**, 417-427
18. Mesak, L. R., Yim, G., and Davies, J. (2009) *Plasmid* **61**, 182-187
19. Mendoza-Vargas, A., Olvera, L., Olvera, M., Grande, R., Vega-Alvarado, L., Taboada, B., Jimenez-Jacinto, V., Salgado, H., Juarez, K., Contreras-Moreira, B., Huerta, A. M., Collado-Vides, J., and Morett, E. (2009) *PLoS One* **4**, e7526
20. Ung, K. S., and Av-Gay, Y. (2006) *FEBS Lett* **580**, 2712-2716
21. San, K. Y., Bennett, G. N., Berrios-Rivera, S. J., Vadali, R. V., Yang, Y. T., Horton, E., Rudolph, F. B., Sariyar, B., and Blackwood, K. (2002) *Metab Eng* **4**, 182-192
22. Zaunbrecher, M. A., Sikes, R. D., Jr., Metchock, B., Shinnick, T. M., and Posey, J. E. (2009) *Proc Natl Acad Sci U S A* **106**, 20004-20009
23. Bajorath, J. (2001) *J Chem Inf Comput Sci* **41**, 233-245
24. Buriankova, K., Doucet-Populaire, F., Dorson, O., Gondran, A., Ghnassia, J. C., Weiser, J., and Pernodet, J. L. (2004) *Antimicrob Agents Chemother* **48**, 143-150
25. Newton, G. L., Buchmeier, N., and Fahey, R. C. (2008) *Microbiol Mol Biol Rev* **72**, 471-494
26. Rawat, M., Newton, G. L., Ko, M., Martinez, G. J., Fahey, R. C., and Av-Gay, Y. (2002) *Antimicrob Agents Chemother* **46**, 3348-3355
27. Sachdeva, P., Misra, R., Tyagi, A. K., and Singh, Y. (2009) *FEBS J* **277**, 605-626
28. Rodrigue, S., Provvedi, R., Jacques, P. E., Gaudreau, L., and Manganelli, R. (2006) *FEMS Microbiol Rev* **30**, 926-941
29. Reeves, R., and Nissen, M. S. (1990) *J Biol Chem* **265**, 8573-8582
30. Smulski, D. R., Huang, L. L., McCluskey, M. P., Reeve, M. J., Vollmer, A. C., Van Dyk, T. K., and LaRossa, R. A. (2001) *J Bacteriol* **183**, 3353-3364
31. Boshoff, H. I., Myers, T. G., Copp, B. R., McNeil, M. R., Wilson, M. A., and Barry, C. E., 3rd. (2004) *J Biol Chem* **279**, 40174-40184
32. Wecke, T., and Mascher, T. (2011) *J Antimicrob Chemother* Sep 19. [Epub ahead of print]
33. Nash, K. A. (2003) *Antimicrob Agents Chemother* **47**, 3053-3060
34. Louw, G. E., Warren, R. M., Gey van Pittius, N. C., Leon, R., Jimenez, A., Hernandez-Pando, R., McEvoy, C. R., Grobbelaar, M., Murray, M., van Helden, P. D., and Victor, T. C. (2011) *Am J Respir Crit Care Med* **184**, 269-276
35. Boshoff, H. I., Xu, X., Tahlan, K., Dowd, C. S., Pethe, K., Camacho, L. R., Park, T. H., Yun, C. S., Schnappinger, D., Ehrt, S., Williams, K. J., and Barry, C. E., 3rd. (2008) *J Biol Chem* **283**, 19329-19341

36. Venketaraman, V., Dayaram, Y. K., Talaue, M. T., and Connell, N. D. (2005) *Infect Immun* **73**, 1886-1889
37. Meighen, E. A. (1991) *Microbiol Rev* **55**, 123-142
38. Green, J., and Paget, M. S. (2004) *Nat Rev Microbiol* **2**, 954-966
39. Ramon-Garcia, S., Ng, C., Anderson, H., Chao, J. D., Zheng, X., Pfeifer, T., Av-Gay, Y., Roberge, M., and Thompson, C. J. (2011) *Antimicrob Agents Chemother* **55**, 3861-3869
40. Snapper, S. B., Melton, R. E., Mustafa, S., Kieser, T., and Jacobs, W. R., Jr. (1990) *Mol Microbiol* **4**, 1911-1919
41. Stover, C. K., de la Cruz, V. F., Fuerst, T. R., Burlein, J. E., Benson, L. A., Bennett, L. T., Bansal, G. P., Young, J. F., Lee, M. H., Hatfull, G. F., and et al. (1991) *Nature* **351**, 456-460
42. Kaps, I., Ehrt, S., Seeber, S., Schnappinger, D., Martin, C., Riley, L. W., and Niederweis, M. (2001) *Gene* **278**, 115-124
43. Murakami, T., Burian, J., Yanai, K., Bibb, M. J., and Thompson, C. J. (2011) *Proc Natl Acad Sci U S A* **108**, 16020-16025

Acknowledgements-J.B. designed, performed and analyzed experiments. S.R.G. designed performed the mycothiol and macrolide preincubation studies, and analyzed data. G.S. assembled the Sweet library and analyzed data. A.G.V. performed mycothiol studies, Y.A. designed and analyzed mycothiol data and interpreted results. C.J.T designed experiments, analyzed data and supervised the work. J.B., S.R.G., G.S., C.J.T. wrote the manuscript. We thank Andrea Basler and Jeffery Hu for technical assistance, Dr. Julian Davies for providing pAmilux and Dr. William Jacobs for providing pMV361.hyg. We thank Dr. Steven Hallam for the use of the Varioskan and qRT-PCR machine and Keith Mewis for technical support with the Varioskan. We also thank Carol Ng, Leah Lim and Quinn Parker for critical reading of the manuscript. This work was supported by Canadian Institute of Health Research grant MOP-82855 held by CJT.

FIGURE LEGENDS

FIGURE 1. Analyses of EGFP and LuxABCDE as reporters of *whiB7* promoter activity. *M. smegmatis* wild type containing A, pMS689GFP or B, pTB674lux treated with 1 μM erythromycin (Ery), 50 μM isoniazid (Iso) or untreated (Untreated). The erythromycin induced fluorescence of pMS689GFP was decreased in the *whiB7* KO (C), a defect that was restored by providing *whiB7 in trans* (D, *whiB7* KO Comp). Signal output from cultures containing E, pGFPon or F, pLUXon in *M. smegmatis* wild type and *whiB7* KO. Values plotted are the mean ± SEM of triplicate samples. Lines are drawn to illustrate trends. Results are representative of multiple transformants.

FIGURE 2. Sites and sequences defining the antibiotic-inducible *whiB7* promoter. A, Alignment of a 60 base pair region 438 to 497 nucleotides upstream of *M. smegmatis whiB7* with sequences from 8 different *Mycobacterium* species. Conserved nucleotides are designated by the star (*) and the mapped transcriptional start site is highlighted by the black box. Here and in the following sections the -10 and -35 regions, and the putative WhiB7 binding site are highlighted in grey. B, Fluorescence response of *EGFP* under the control of shortened *whiB7*-promoter regions, pMS497GFP and pMS483GFP, in *M. smegmatis* either untreated or treated with 1 μM erythromycin (+ery). Values plotted are the mean ± SEM of triplicate samples. Lines illustrate the trend. Results are representative of multiple transformants. C, The transcription start site was mapped using RT PCR (19) and the transcript cloned. The sequences of two independent clones (bottom) were aligned to the *M. smegmatis* genome sequence (top). The matching sequence is boxed, the transcriptional start site is marked TSS. D, An alignment of the identified *whiB7* promoter motif across 13 genera of actinomycetes. The variable distance from the start codon is boxed E, The putative WhiB7 binding site and promoter motif is present upstream of several *M. tuberculosis* H37Rv genes within the WhiB7 regulon as well as *erm(38)* the ortholog of *ermMT* in *M. smegmatis*.

FIGURE 3. Structural comparison of identified *whiB7* promoter activators. Identified activators were clustered according to chemical structure similarity using PubChem (http://pubchem.ncbi.nlm.nih.gov/assay/assay.cgi?p=clustering). A Tanimoto score of ≥0.7 is indicative of highly similar structure with potentially similar bioactivity. Numerous activators clustered within distinctive structural classes are highlighted (blue, macrolides; red, aminoglycosides; yellow, fluoroquinolones; green, tetracyclines). Activators confirmed by qRT-PCR are indicated by a red star (*).

FIGURE 4. The *whiB7* promoter responds to the toxic macrolide-ribosome interaction. *M. smegmatis* wild type and *ermMT* OE carrying pMS689GFP were treated with 1.85 μM erythromycin (Ery), 0.62 μM dirithromycin (Diri), 0.62 μM roxithromycin (Roxi), 0.62 μM azithromycin (Azi), or 0.069 μM doxycycline (Doxy) for 5 hours and the fluorescence compared to untreated cultures. All drugs were pretested to define their most effective concentrations for *whiB7* induction in *M. smegmatis* wild type. Values plotted are the mean ± SEM of three biologically independent experiments.

FIGURE 5. *whiB7* promoter activation is altered by intracellular redox. A, Increase of *whiB7* mRNA in cultures treated with 8 μM erythromycin (Ery8), 1 μM erythromycin (Ery1), 1 μM erythromycin under reducing conditions (10 mM DTT + Ery1), 1 μM erythromycin under oxidizing conditions (Diamide (5 mM) + Ery1), reducing conditions (DTT (10 mM)) or oxidizing conditions (Diamide (5 mM)) relative to a non-treated control. Results plotted are the mean ± SEM of duplicate measurements and representative of three experiments. B, The reduced form (MSH) and the oxidized disulfide form (MSSM) of mycothiol were quantified in *M. smegmatis* wild type or *whiB7* KO. Cultures were either untreated (Untreated) or treated for 1 hour with 256 μg/mL erythromycin (Erythromycin). Results plotted are the mean ± SEM of three biologically independent experiments. C, The redox ratio (MSH:MSSM) was calculated from mycothiol quantities (plotted in 'B') of untreated (Untreated) or 256 μg/mL erythromycin treated (Erythromycin) *M. smegmatis* wild type or *whiB7* KO strains. Values are the mean ± SEM.

TABLE

TABLE 1. Strains and plasmids used

Strains	Description	Reference
Mycobacterium smegmatis mc^2155		
wild type	Unmodified lab strain	(40)
whiB7 KO	Genomic region 2031710 to 2032094 (containing *MSMEG_1953* (*whiB7*)) replaced by Hygromycin resistance; Hyg^R	(CJT, SRG unpublished)[a]
ermMT OE	pERM.hyg integrated into genome constitutively expressing *ermMT* to provide macrolide resistance; Hyg^R	This Study
whiB7 KO Comp	p361comp.apra integrated into the genome of the *whiB7* KO strain providing *whiB7* expressed under its own promoter *in trans*; Hyg^R $Apra^R$	This Study
Plasmids		
pLUXon	Constitutively expressed *luxABCDE* using HSP60 promoter in the integrative vector pMV361; Kan^R	This Study
pTB674lux	*luxABCDE* controlled by the *M. tuberculosis whiB7* promoter region (up to 674 nucleotides upstream of Rv3197a) replacing the HSP60 promoter in the integrative vector pMV361; Kan^R	This Study
pGFPon	Constitutively expressed *EGFP* using HSP60 promoter on the multi-copy vector pMV261; Kan^R	This Study
pMS689GFP	*EGFP* controlled by the *M. smegmatis whiB7* promoter (up to 689 nucleotides upstream) in the promoterless, multi-copy pMycVec1	This Study

	vector; Kan^R	
pMS497GFP	*EGFP* controlled by the *M. smegmatis whiB7* promoter (up to 497 nucleotides upstream) in the promoterless, multi-copy pMycVec1 vector; Kan^R	This Study
pMS483GFP	*EGFP* controlled by the *M. smegmatis whiB7* promoter (up to 483 nucleotides upstream) in the promoterless, multi-copy pMycVec1 vector; Kan^R	This Study
pMS438GFP	*EGFP* controlled by the *M. smegmatis whiB7* promoter (up to 438 nucleotides upstream) in the promoterless, multi-copy pMycVec1 vector; Kan^R	This Study
pERM.hyg	Constitutively expressed *ermMT* (Rv1958) using HSP60 promoter in the integrative vector pMV361.hyg; Hyg^R	This Study
p361comp.apra	Modified pMV361 vector with the HSP60 promoter replaced by *whiB7* under its own promoter and kanamycin resistance replaced by apramycin resistance; $Apra^R$	This Study
pMV361	Integrative vector containing kanamycin resistance, integrase gene and the HSP60 promoter upstream of a multiple cloning site	(41)
pMV261	Multicopy vector containing kanamycin resistance and the HSP60 promoter upstream of a multiple cloning site	(41)
pMV361.hyg	Modified pMV361 with kanamycin resistance replacing hygromycin resistance	(41)
pMycVec1	Multicopy vector containing kanamycin resistance and promoterless multiple cloning site	(42)
pAB707	Source of the apramycin resistance gene aac(3)IV	(43)

[a]Construction and further complementation of the *whiB7* KO is to be published elsewhere

Hyg^R = hygromycin resistance Kan^R= hygromycin resistance $Apra^R$ = apramycin resistance

TABLE 2. Comparison of *whiB7* transcriptional activators to the *whiB7* resistance spectrum.

Compound	MIC (μM)[a]		Fold increase in susceptibility	Fold increase [b] of *whiB7* mRNA (treatment concentration in μM)[c]
	wild type	*whiB7* KO		
erythromycin stearate	32	2	16	324 (1)
retapamulin	100	6.25	16	657 (50)
capreomycin	3	1.5	2	24 (1.9)
tilmicosin	1.5	0.75	2	47 (1.85)
doxycycline hyclate	0.5	0.25	2	1860 (0.21)
amikacin	1	1-0.5	1-2	100 (16.7)
dequalinium	0.78	0.78	1	38 (1.85)
linezolid	0.375	0.375	1	142 (1.9)
danofloxacin	0.75	0.75	1	31 (16.7)
acivicin	>800	>800	-	65 (50)
A23187	>25	>25	-	593 (5.56)
erythromycin	16-32	nd	-	94 (1)
isoniazid	116-232	nd	-	0.3 (50)

[a]MICs were determined in three biologically independent samples.
[b]Fold increase in mRNA (ratio of treated/ untreated) was determined from a sample analyzed in duplicate after 3 hours of induction (concentration shown in brackets).
[c]Concentrations correspond to the highest fold increase of pMS689GFP fluorescence in the chemical screen.
nd = not determined

Figure 1

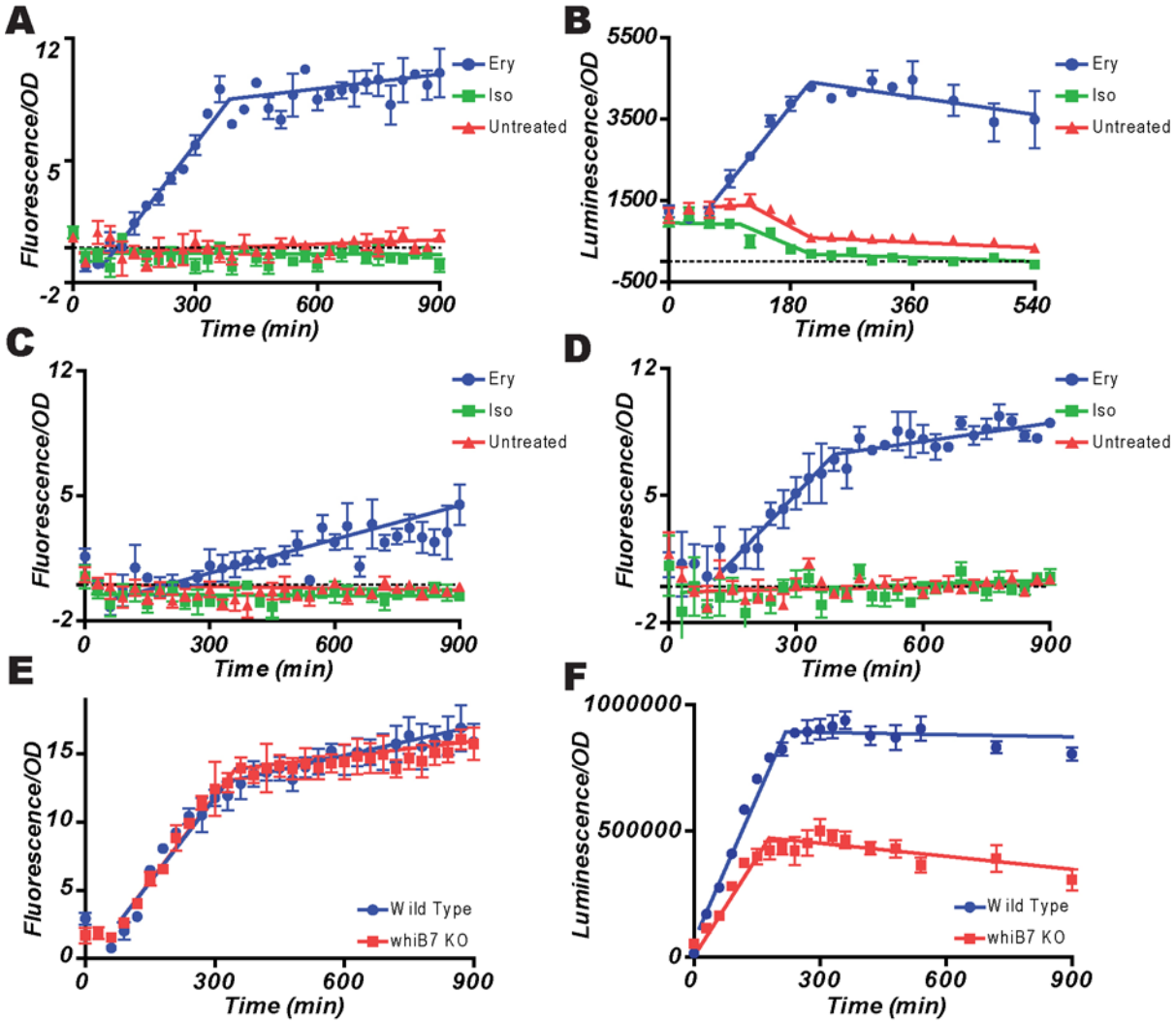

Figure 2

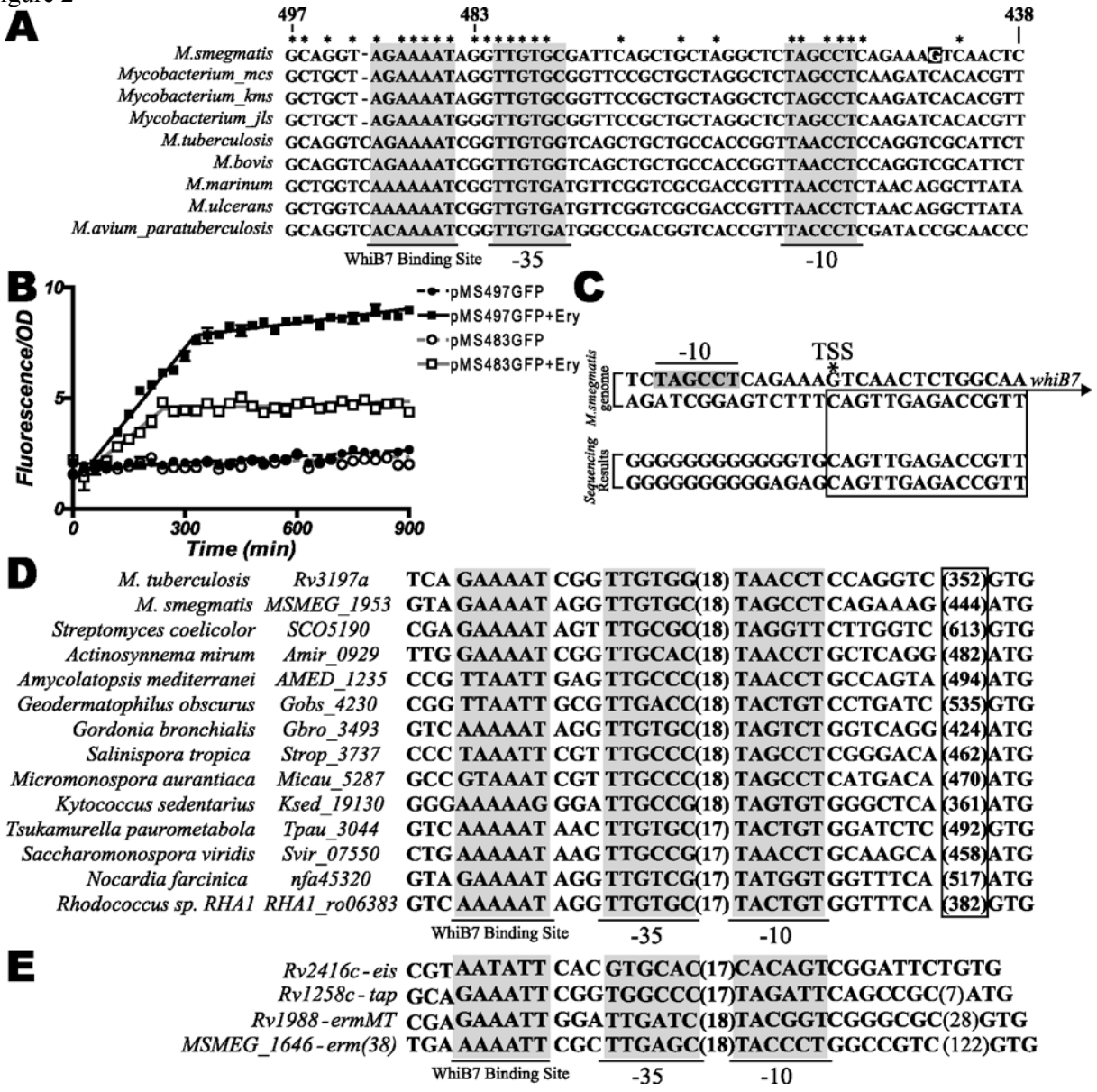

Figure 3

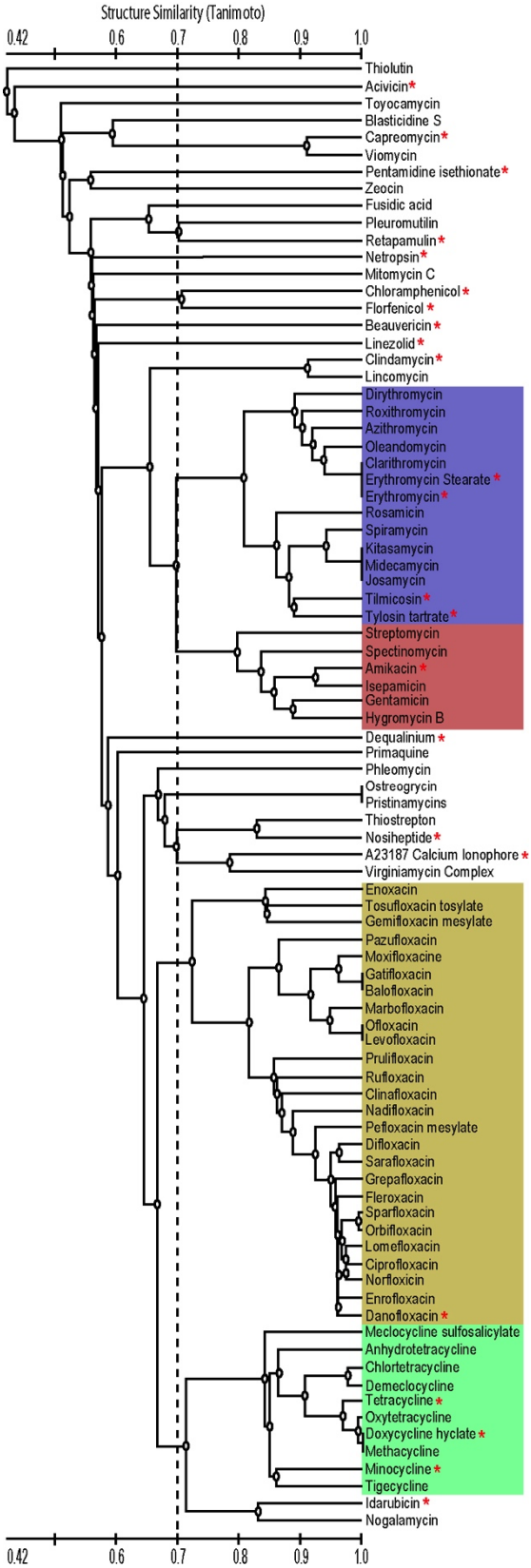

Figure 4

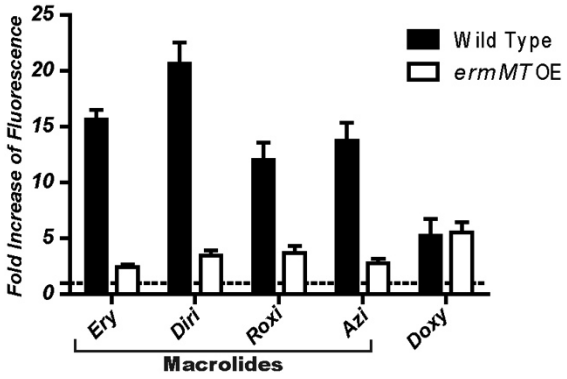

Figure 5